J. Neural Eng. **6** (2009) 046007 (10pp) doi:10.1088/1741-2560/6/4/046007

Decentralized adaptive robust control based on sliding mode and nonlinear compensator for the control of ankle movement using functional electrical stimulation of agonist–antagonist muscles

Hamid-Reza Kobravi and Abbas Erfanian

Iran Neural Technology Research Centre, Department of Biomedical Engineering, Faculty of Electrical Engineering, Iran University of Science and Technology, Narmak, 16846, Tehran, Iran

E-mail: erfanian@iust.ac.ir

Received 4 September 2008
Accepted for publication 9 June 2009
Published 9 July 2009
Online at stacks.iop.org/JNE/6/046007

Abstract

A decentralized control methodology is designed for the control of ankle dorsiflexion and plantarflexion in paraplegic subjects with electrical stimulation of tibialis anterior and calf muscles. Each muscle joint is considered as a subsystem and individual controllers are designed for each subsystem. Each controller operates solely on its associated subsystem, with no exchange of information between the subsystems. The interactions between the subsystems are taken as external disturbances for each isolated subsystem. In order to achieve robustness with respect to external disturbances, unmodeled dynamics, model uncertainty and time-varying properties of muscle-joint dynamics, a robust control framework is proposed which is based on the synergistic combination of an adaptive nonlinear compensator with a sliding mode control and is referred to as an adaptive robust control. Extensive simulations and experiments on healthy and paraplegic subjects were performed to demonstrate the robustness against the time-varying properties of muscle-joint dynamics, day-to-day variations, subject-to-subject variations, fast convergence, stability and tracking accuracy of the proposed method. The results indicate that the decentralized robust control provides excellent tracking control for different reference trajectories and can generate control signals to compensate the muscle fatigue and reject the external disturbance. Moreover, the controller is able to automatically regulate the interaction between agonist and antagonist muscles under different conditions of operating without any preprogrammed antagonist activities.

(Some figures in this article are in colour only in the electronic version)

1. Introduction

Over the past three decades, many research groups have shown that limited restoration of function to paralyzed limbs can be achieved through functional neuromuscular stimulation (FNS). This technology has been used to restore hand grasp and elbow extension in individuals with tetraplegia [1–3], to provide standing and locomotion for paraplegic subjects [4, 5] and to correct drop foot in subjects with an upper motor neuron lesion (due to stroke, incomplete spinal cord injury, multiple sclerosis, cerebral palsy and head injury) [6]. In FNS systems, sequences of current pulses excite the intact peripheral axons, which in turn contract paralyzed muscles. By changing the pulse width, pulse amplitude or pulse frequency, the level of contraction can be altered to perform a specific task. To provide functional use of the paralyzed limbs, an appropriate electrical stimulation pattern should be delivered to a set of muscles.

A major impediment to stimulating the paralyzed neuromuscular systems and determining the stimulation pattern has been the highly nonlinear, time-varying properties of electrically stimulated muscle, muscle fatigue, spasticity and day-to-day variations which limit the utility of a pre-specified stimulation pattern and an open-loop FNS control system. To deal with these problems, many control strategies have been developed and reported in the literature including a fixed-parameter feedback controller [7, 8], adaptive feedback techniques [9–12], fixed-parameter feedforward [13, 14], adaptive feedforward [14–19] and combination of feedforward and feedback control techniques [13–15, 20].

All these works indicate that tracking quality was improved by the use of the adaptive control law compared to the non-adaptive one. An adaptive control, by online tuning the parameters (of either the plant or the controller—corresponding to the indirect, or direct adaptive control), can deal with uncertainties, but generally, suffers from the disadvantage of being able to achieve only *asymptotical* convergence of the tracking error to zero. The basic idea in adaptive control is to estimate the uncertain plant parameters (or, equivalently, the corresponding controller parameters) online based on the measured systems signal, and use the estimated parameters in the control input computation. Generally, this algorithm is based on the assumption that the structure of the system model is known with unknown system slow-varying parameters and the parameters appear linear. Several issues, such as transient performance, unmodeled dynamics, disturbance, the amount of offline training, the tradeoff between the persistent excitation of signals for correct identification and the steady system response for control performance, the model convergence and system stability issues in real applications and nonlinearity in parameters, often complicate the adaptive approach [21–23].

A useful and powerful control scheme to deal with the uncertainties, nonlinearities and bounded external disturbances is sliding mode control (SMC) [24]. In robust control designs, a fixed control law based on *a priori* information on the uncertainties is designed to compensate for their effects, and *exponential* convergence of the tracking error to a (small) ball centered at the origin is obtained. The robust control has some advantages over the adaptive control, such as its ability to deal with disturbances and quickly varying parameters [24]. Nevertheless, the SMC suffers from high-frequency oscillations in the control input, which is called 'chattering' [25, 26]. Chattering is undesirable because it can excite unmodeled high-frequency plant dynamics.

The SMC has already been used for the control of FES [27, 28] in human subjects. Jezernik *et al* [27] reported the use of a sliding mode closed-loop controller for the control of knee-joint angle by stimulating the quadriceps muscle. To reduce the chattering, they replaced the discontinuous term by a continuous one in the sliding control law. In this case, the controller cannot force the system into a sliding-mode regime and does not ensure robustness and good tracking performance [29]. In previous work [28], we designed a control methodology which is based on the synergistic combination of artificial neural networks with SMC. A recurrent neural network was used to model the uncertainties and to provide an auxiliary equivalent control to keep the uncertainties to low values and consequently to use a SMC with lower switching gain. The method was designed for the control of knee-joint angle using single muscle group (i.e. quadriceps muscle) stimulation. However, extension of the work to multiple muscle systems (e.g. simultaneous co-activation of agonist and antagonist muscles) remains an open problem. Moreover, initial evaluation of the conventional SMC for the control of human gait [30] and high-order sliding modes (HOSMs) for the control of multiple muscle systems in a single joint [31] were performed in a simulation-based study. Although the chattering can be removed by properly using HOSMs, the main problem in the implementation of HOSMs is increasing information demand. The parameters of the HOSM controller should satisfy certain conditions in order to guarantee the finite-time convergence. These conditions highly depend on the information about the system which is not easily available. Another drawback of HOSMs is revealed when the relative degree r of the measurable sliding variable s is higher than 1, as they generally require knowledge of its derivatives up to the $(r-1)$th order. Unfortunately, the problem of successive real-time exact differentiation is considered to be practically unsolvable and derivatives must be estimated by means of some observers (e.g. 'high-gain' observer or sliding differentiator) [32].

In order to limit the chattering phenomena and to preserve the main advantages of the original SMC, we propose a new control strategy which is based on SMC, fuzzy logic systems and adaptive control, referred to as adaptive robust control (ARC), for controlling the ankle movement in paraplegic subjects using agonist–antagonist co-activation.

Another important issue in the design of FNS control systems is that a large number of muscles need to be stimulated to coordinate several degrees of freedom of movements. The controller has to cope with a significant coupling existing among individual joints. The controller must also intelligently assign activations to agonist and antagonist muscles with the goal of achieving the beneficial effects of co-contraction during normally occurring movement [33, 34]. Centralized controller design of such a system requires a complex mathematical model of musculoskeletal dynamics in the control law formulation [35–38]. This approach is computationally intensive and the performance of the control system is ultimately governed by the fidelity of the mathematical model used to describe the musculoskeletal dynamics. Controller complexity can be considerably reduced if decentralized control schemes are used. The decentralized control problem is to design a set of independent controllers in which each subsystem is controlled by a stand-alone controller [39]. Each controller, developed based only on local information and measurements, operates solely on its associated subsystem. The interaction between the subsystems is taken as external disturbances for each isolated subsystem.

In this work, we present a new decentralized control strategy which is based on ARC for the control of ankle movement while the agonist (antagonist) muscle joint is considered as a subsystem.

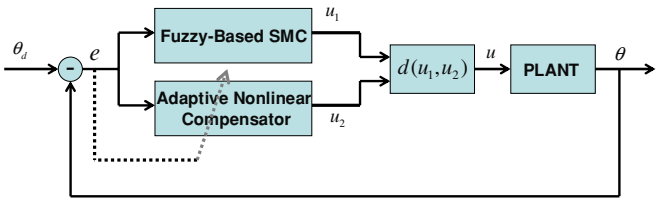

Figure 1. Structure of the proposed adaptive robust control.

2. Methods

2.1. Structure of an ARC

Although sliding mode control (see the appendix for details) has long being known for its capabilities in achieving robust control; it also suffers from large control chattering that may excite the unmodeled high-frequency response of the systems due to the discontinuous switching and imperfect implementations. One commonly used method to eliminate the effects of chattering is to replace the switching control law by a saturating approximation [24] within a boundary layer around the sliding surface. Inside the boundary layer, the discontinuous switching function is approximated by a continuous function to avoid discontinuity of the control signals. Even though the boundary layer design can alleviate the chattering phenomenon, these approaches, however, provide no guarantee of convergence to the sliding mode [29] and involve a tradeoff between chattering and robustness, and result in the existence of the steady-state error. In order to limit the chattering phenomena and to preserve the main advantages of the original SMC, we propose a new SMC by combining an adaptive nonlinear compensator with the SMC. The configuration of the proposed control strategy is schematically depicted in figure 1, where u_1 is the output of the SMC defined in [(A.8)], u_2 is the output of an adaptive nonlinear compensator as the auxiliary control input (defined in section 2.1) and $u = d(u_1, u_2)$ is a function of u_1 and u_2 defined by

$$u = d(u_1, u_2) = \begin{cases} u_1 & \text{if} \quad |s(e)| > \phi \\ \alpha(e)u_1 + (1-\alpha(e))u_2 & \text{if} \quad |s(e)| \leqslant \phi, \end{cases} \tag{1}$$

where $s(e)$ is a scalar function described in [(A.5)], ϕ is the boundary layer thicknesses and $\alpha(e)$ is a function of error and is adapted by

$$\alpha(e) = \frac{|s(e)|}{\phi}. \tag{2}$$

The original SMC structure is retained in the proposed scheme, but the role of adaptive nonlinear compensator becomes more significant as the state trajectory is nearing the sliding surface.

2.2. Adaptive nonlinear compensator (ANC)

In order to guarantee the closed-loop stability and minimize the tracking error inside the boundary layer, an adaptive nonlinear compensator is proposed whose output is combined with the output of the SMC when the state trajectory of a system enters some boundary layer around the sliding surface, i.e.

$$\begin{aligned} \kappa &= \left(\frac{\mathrm{d}}{\mathrm{d}t} + 1\right)^2 \left(\int_0^t e \,\mathrm{d}r\right) \\ u_2 &= f\left(e, \dot{e}, \int e \cdot \mathrm{d}t\right) = \alpha \cdot \tan h(\beta \cdot (\kappa - \gamma)), \end{aligned} \tag{3}$$

where e is the state error. The parameters $\rho = (\alpha, \beta, \gamma)$ are adapted online during the online control without offline training such that the system output θ can asymptotically track the desired output θ_d. In order to derive an adaptation mechanism that would guarantee the global asymptotic stability of the control system, we choose the Lyapunov function candidate

$$V = \tfrac{1}{2} \cdot (\theta - \theta_d)^2 = \tfrac{1}{2} \cdot e^2. \tag{4}$$

Based on the Lyapunov theorem, if a control input u_2 can be chosen to satisfy $\dot{V} \leqslant 0$, then the function V will be monotonically decreasing for time $t \geqslant 0$. By using the following adaptation rule, it was proved that the output tracking error asymptotically converges to zero [40]:

$$\dot{\rho} = -\delta \cdot e \cdot \frac{\partial u_2}{\partial \rho} \cdot \mathrm{sgn}\left(\frac{\partial \theta}{\partial u}\right), \tag{5}$$

where $\delta > 0$ is the learning rate parameter and $\mathrm{sgn}(\cdot)$ is a sign function.

2.3. Fuzzy-based SMC

To implement the SMC, the nonlinear function $f(x)$ and the control gain $g(x)$ in [(A.1)] should be estimated. In this work, we use a fuzzy logic system to approximate the nonlinear function $f(x)$. An interesting and tempting authority of fuzzy logic systems is their capability for approximating various types of nonlinear functions. It was proved that certain classes of fuzzy logic system have universal approximation ability [41]. The fuzzy system uses the fuzzy IF–THEN rules to perform a mapping from an input vector $x = [x_1, x_2, \ldots, x_n]^T \in \Re^n$ to an output $\hat{f}(x) \in \Re$. The rth fuzzy rule is written as

$$R^r : \text{if } x_1 \text{ is } A_1^r(x_1) \text{ and} \ldots \text{and } x_n \text{ is } A_n^r(x_n), \text{ then } y \text{ is } B^r,$$

where A_i^r and B_i^r are the fuzzy sets with the membership functions $\mu_{A_i^r}(x_i)$ and $\mu_{B^i}(y)$, respectively, and x belongs to a compact set. By using the product–inference rule, singleton fuzzifier and center-average defuzzifier, the output of FLS can be expressed as

$$\hat{f}(x) = \frac{\sum_{i=1}^{n_r} \tilde{y}^i \left(\prod_{j=1}^{n} \mu_{A_j^i}(x_j)\right)}{\sum_{i=1}^{n_r} \left(\prod_{j=1}^{n} \mu_{A_j^i}(x_j)\right)} = \vartheta^T \psi(x), \tag{6}$$

where n_r is the number of total fuzzy rules, $\tilde{y}^i$ is the fuzzy singleton for the output in the ith rule, $\mu_{A_j^i}(x_j)$ is the membership function of the fuzzy variable x_j characterized by the Gaussian function, $\vartheta = [\tilde{y}^1, \tilde{y}^2, \ldots, \tilde{y}^{n_r}]^T$ is an adjustable parameter vector and $\psi = [\psi^1, \psi^2, \ldots, \psi^{n_r}]^T$ is a fuzzy basis vector, where ψ^i is defined as

$$\psi^i(x) = \frac{\left(\prod_{j=1}^{n} \mu_{A_j^i}(x_j)\right)}{\sum_{i=1}^{n_r} \left(\prod_{j=1}^{n} \mu_{A_j^i}(x_j)\right)}. \tag{7}$$

In this work, we use the standard recursive least-squares (RLS) algorithm to estimate the parameters ϑ and g.

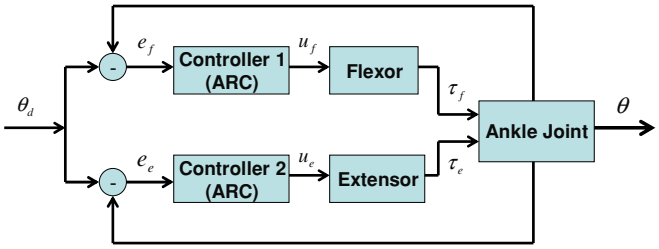

Figure 2. Decentralized adaptive robust control system of ankle movement.

2.4. Decentralized control of ankle movement using agonist–antagonist co-activation

A representative diagram of the proposed control system of ankle movement is shown in figure 2. Each muscle joint has its own controller developed in sections 2.1 and 2.2. To implement ARC, the musculoskeletal system should be presented in a standard canonical form as

$$\ddot{\theta} = f_f(\theta, \dot{\theta}) + g_f \cdot u_f(t) + w_f(t) \tag{8}$$

$$\ddot{\theta} = f_e(\theta, \dot{\theta}) + g_e \cdot u_e(t) + w_e(t), \tag{9}$$

where (8) and (9) present muscle-joint dynamics for dorsiflexion and plantarflexion movements, respectively. The parameter θ denotes the ankle angle, θ and $\dot{\theta}$ are the system states and u_f and u_e are the input commands to the dorsiflexor and plantarflexor muscles, respectively. w_f and w_e represent dynamic coupling, parameter uncertainty, unmodeled dynamics, gravity loading of the musculoskeletal system and external disturbances for the dorsiflexion and plantarflexion, respectively. The error signals used for controllers of two muscles are calculated as

$$\begin{bmatrix} e_e \\ e_f \end{bmatrix} = \begin{bmatrix} +1 \\ -1 \end{bmatrix} [\theta - \theta_d] \tag{10}$$

where e_f and e_e are the error signals for controllers of the flexor and extensor, respectively; θ is the measured joint angle, and θ_d is the desired trajectory.

The fuzzy modeling approach is used to approximate the nonlinear functions $f_f(\theta, \dot{\theta})$ and $f_e(\theta, \dot{\theta})$. Offline identification of the fuzzy models, g_f and g_e parameters, are performed by the RLS algorithm using a pulse-width-modulation random sequence. To generate a random stimulation signal, a random sequence of pulse widths with a uniform distribution is passed through a Butterworth low-pass digital filter with a cutoff frequency of $\omega_c = 5$ Hz. During experimental evaluation, muscle-joint dynamics for the dorsiflexion and plantarflexion were identified through two separate experimental trials during the first experiment session on a healthy subject and then used for subsequent experiments on different days and all subjects.

3. Simulation studies

A musculoskeletal model which was presented in [15] is used here as a virtual patient in simulation studies. The model of electrically stimulated muscle used in this study includes nonlinear recruitment, linear dynamics and multiplicative nonlinear torque–angle and torque–velocity scaling factors. The virtual patient consists of a single skeletal segment in a swing pendulum configuration with one degree-of-freedom. The skeletal segment is acted upon by an agonist–antagonist pair of electrically stimulated muscles. The set of parameters for muscle and skeletal models are taken from [15].

We use the root-mean-square (RMS) error and normalized RMS (NRMS) as the performance indices for measuring the tracking accuracy as follows:

$$\text{RMS} = \sqrt{\frac{1}{T}\sum_{t=1}^{T}(\theta(t) - \theta_d(t))^2} \tag{11}$$

$$\text{NRMS} = \frac{1}{(\theta_{\max} - \theta_{\min})}\sqrt{\frac{1}{T}\sum_{t=1}^{T}(\theta(t) - \theta_d(t))^2} \times 100. \tag{12}$$

The SMC parameters (i.e. k, ϕ and λ) are chosen heuristically to achieve the best controller performance during simulation studies. Of course, there are some guidelines for choosing the SMC parameters [28]. The SMC would require using a high switching gain, k, in order to compensate for the effects of uncertainties. This would also lead to the use of a thicker boundary layer in order to eliminate the higher chattering effect resulting from the use of a high switching gain. Although the chattering behavior can be reduced by increasing the boundary layer thickness, the control system is actually changing to a system without a sliding mode when a thick boundary layer is used. According to these guidelines, the parameters of the proposed SMC were selected as follows:

$$k = 50, \qquad \phi = 5, \qquad \lambda = 3.$$

Figures 3(a)–(c) show the results of the conventional SMC of the ankle joint angle in a virtual patient for different values of a boundary layer width (i.e. ϕ) with $k = 50$ and $\lambda = 3$. It is clearly observed the high control activity and the chattering due to the SMC (figure 3(a), RMS error 5.4° (6.75%)). Increasing the boundary layer thickness reduces chattering but increases the tracking error (figure 3(b): RMS error 6.9° (8.63%), figure 3(c): RMS error 10.0° (12.50%)).

The result of the ankle movement control using the proposed ARC, with $k = 50$, $\phi = 5$ and $\lambda = 3$, is shown in figure 3(d) (RMS error 0.79° (0.99%)). It is observed that the chattering of control signals produced by the SMC is effectively eliminated even with a thinner boundary layer. It is apparent that the proposed control strategy is able to provide remarkably fast and robust tracking with a smooth control action. The interesting observation is the presence of antagonist co-activation during ankle movement. At the low levels of activation, both muscles are engaged. The activity of antagonist (agonist) decreases as agonist (antagonist) activity increases. At the peak angles, there is no overlap between the agonist and antagonist muscles. The agonist–antagonist overlap is about 22.5%. It has already been shown that through the use of electrical stimulation under various nonisometric conditions, a moderate application of

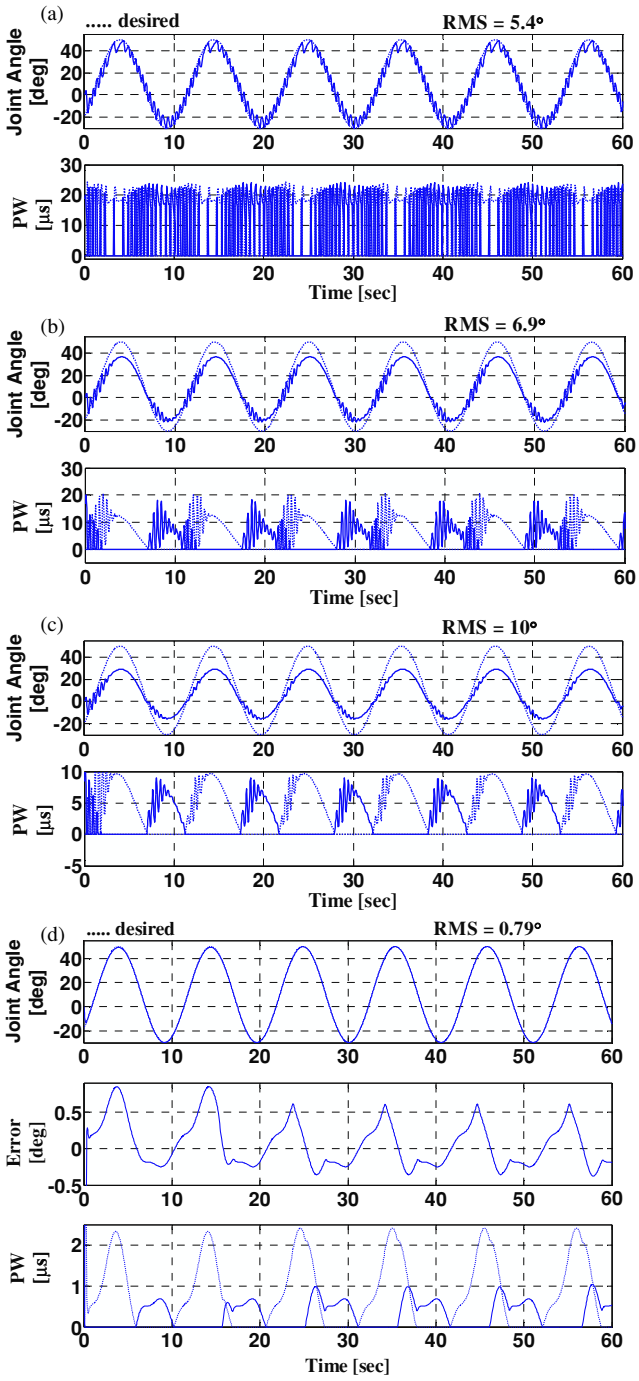

Figure 3. Simulation results of the ankle movement control obtained by the conventional SMC ($k = 50$, $\lambda = 3$) with boundary layer thicknesses $\phi = 0$ (a), $\phi = 10$ (b) and $\phi = 15$ (c). Simulated responses of the ARC ($k = 50$, $\lambda = 3$) with boundary layer thickness $\phi = 5$ (d). The controller forces the output of the plant to exactly track the desired trajectory. The bottom plots in (a)–(d) show the control outputs of agonist (solid) and antagonist (dotted).

antagonistic activity between 25% and 50% overlap does not significantly deteriorate the range of motion, and it has the potential to reduce the occurrence of long-term pathologic joint laxity and, thereby, maintain joint stiffness at low force ranges [33]. It is note worthy that co-activation activity is automatically adjusted by the control strategy without predefining a co-activation map.

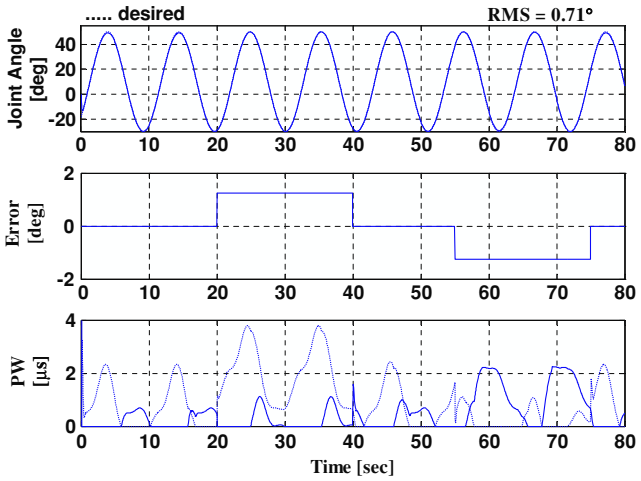

Figure 4. Simulation results of an external disturbance rejection using the proposed SMC ($k = 50$, $\phi = 5$, $\lambda = 3$). A constant torque in amount of 1.25 Nm (which is approximately 50% of the peak-to-peak generated torque during the disturbance-free trial) was added to and subtracted from the net torque generated by the two muscles for a duration of 30 s. The level of co-activation is 22.5% during the disturbance-free trial, while it increases to 44.0% during the positive disturbance and to 43.0% during the negative disturbance. The bottom plot shows the control outputs of agonist (solid) and antagonist (dotted).

3.1. Effects of external disturbances

To evaluate the ability of a proposed control strategy to external disturbance rejection, a constant torque amount of 1.1 Nm (which is approximately 50% of the peak-to-peak generated torque during the disturbance-free trial) was added to and subtracted from the net torque generated by the two muscles for a duration of 20 s at 20 s and 55 s, respectively. Figure 4 shows that excellent tracking performance and fast convergence speed can be achieved under external disturbances using the proposed SMC (RMS error 0.71° (0.89%)). It is interesting to note that the level of co-activation increases as the level of muscle activation increases. This may be explained by what was recorded from normal human subjects [33, 34]. The co-activation strategies recorded from normal humans show that as increased net joint torque is required, the antagonist activity increases, albeit at a much lesser rate than the agonist. The level of co-activation is 22.5% during disturbance-free duration, while it increases to 44.0% during positive disturbance and to 43.0% during negative.

3.2. Effects of muscle fatigue

In FNS applications, muscle fatigue can cause degradation of system performance. To evaluate the ability of the controller to account for muscle fatigue, the effects of muscle fatigue were simulated by an asymptotic decrease in the agonist's (antagonist's) input gain to 40% (42%) of its original value over 180 s. Figure 5 demonstrates that the proposed SMC can provide a very good tracking performance during muscle fatigue (RMS error is 1.66° (3.32%) over 120 s). The controller could adjust the stimulation pattern to achieve a consistent tracking performance. The interesting observation is that by

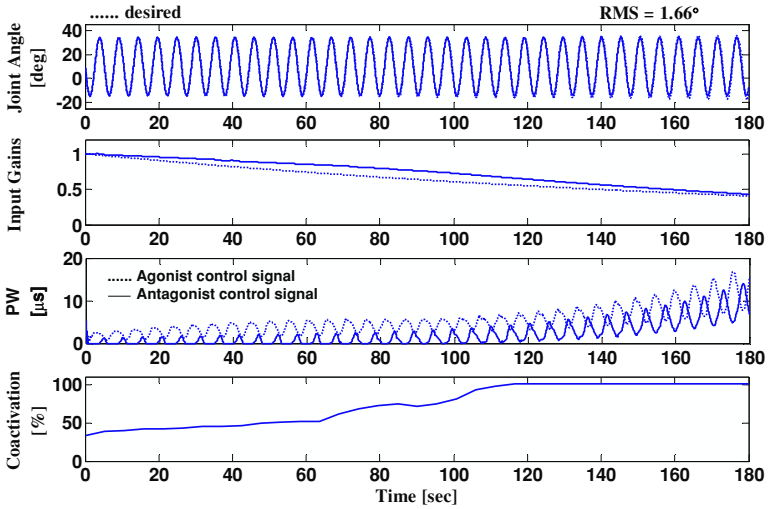

Figure 5. Simulation result of fatigue compensation obtained by the ARC ($k = 50, \phi = 5, \lambda = 3$). The effects of muscle fatigue were simulated by exponentially decreasing the muscle input gain during the course of the simulation. Muscle's input gains have been reached to 40% and 42% of their initial value after 180 s for agonist and antagonist muscles, respectively.

increasing the agonist activity during fatigue, the antagonist activity increases. The level of co-activation increases as the muscles becomes fatigued.

4. Experimental evaluation

4.1. Experimental procedure

The experiments were conducted on three intact persons and three thoracic-level complete spinal cord injury subjects with injury at T7 and T12 levels using an eight-channel computer-based closed-loop FNS system [42]. The paraplegic subjects were active participants in a rehabilitation research program involving daily electrically stimulated exercise of their lower limbs (either seated or during standing and walking) using ParaWalk neuroprosthesis [43]. All experimental procedures were approved by the local ethics committee and the subject gave informed consent. The subject was seated on a bench with his hip flexed at approximately 90° and the knee joint positioned at 0°, while the ankle was allowed to plantarflexing and dorsiflexing. The tibialis anterior and calf muscles were stimulated using adhesive surface elliptical electrodes (5 × 10 cm GymnaUniphy electrodes, COMEPA Industries, Belgium). Pulse width modulation (from 0 to 700 μs) with balanced bipolar stimulation pulses, at a constant frequency (25 Hz) and constant amplitude, was used. The controller adjusted the pulse widths and pulse widths with a negative value were then set to zero. An electrogoniometer (model SG150, Biometrics Ltd, Gwent, UK) was fixed on the ankle joint to measure the ankle-joint position. The measured signals were sampled at 1 kHz by a 12 bit analog-to-digital converter (Advantech PCI-1711 I/O card).

The computer-based closed-loop FNS system uses Matlab Simulink (The Mathworks, R2007b), Real-Time Workshop and Real-Time Windows Target under Windows 2000/XP for online data acquisition, processing and controlling. The proposed control strategy was implemented by the S-functions using C^{++}.

Three different types of desired movement trajectories were used to evaluate the stability and tracking the performance of the proposed strategy. The first pattern has a biphasic trapezoidal stimulation intensity envelope with a period of 20 s and a duty cycle of 60% (12 s on (movement phase) and 6 s off (rest phase)). The second one is a biphasic raised-cosine with a period of 12 s and a duty cycle of 50% (6 s on (movement phase) and 6 s off (rest phase)). The third stimulation pattern has a sine-wave envelope with a period of 20 s. The range of motion is between $-10°$ and 32°. During each experiment day, five trials were conducted on each subject and inter-trial resting intervals of at least 5 min were used. The duration of each trial is 120 s for a normal test and 180 s for a fatigue test.

The parameters of the controller during experimental evaluation were set at the same values used during simulation.

4.2. Experimental results

Figure 6 shows typical results of identifying the muscle-joint models (16) and (17) for dorsiflexion and plantarflexion movements in an intact subject using the fuzzy logic system. The values of the identified parameters were used for subsequent experiments on different days for all intact and paraplegic subjects. The able-bodied individuals were instructed not to try to move their lower limbs during experiments. Examples of joint angle trajectories obtained with the proposed SMC on all subjects are shown in figure 7. Excellent tracking performance with no chattering is achieved using the proposed control strategy. The most interesting observation is the fast convergence speed of the proposed control strategy. The ankle movement trajectory converges to the desired trajectory after about 2 s. It should be noted that the values of the model parameters (16) and (17) for all subjects and all experiment days are set the same values which were determined during the first experiment day on one

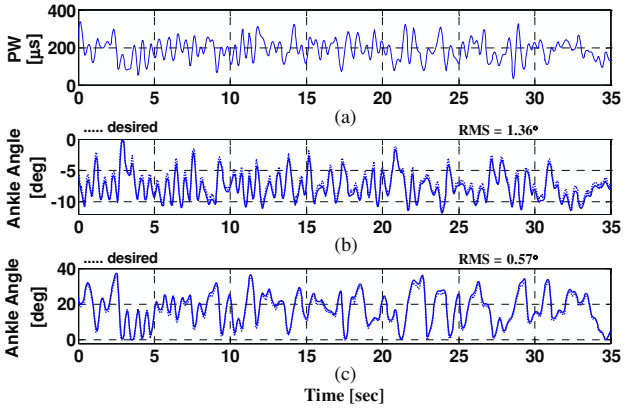

Figure 6. Measured (solid line) and predicted (dotted line) joint angle obtained using identified ankle-joint dynamics in an intact subject using random electrical stimulation (a) of plantarflexor (b) and dorsiflexor (c) muscles.

Table 1. Summary of the average daily root-mean-square tracking error (±standard deviation) obtained for healthy subjects using the ARC.

Subject	Day 1	Day 2	Day 3
KM	2.27° ± 0.30°	4.02° ± 0.20°	3.33° ± 0.27°
NH	2.32° ± 0.34°	3.28° ± 0.60°	2.95° ± 0.93°
AS	5.59° ± 0.25°	4.28° ± 0.52°	4.72° ± 1.53°
Mean		3.20° ± 1.20°	

intact person and updating the parameters of adaptive nonlinear compensator is performed online without any offline training.

A summary of results over 90 trials on all subjects over three days (tables 1 and 2) indicates that the proposed control strategy is able to achieve and maintain perfect tracking performance by rapidly adapting the stimulation pattern. The average RMS tracking error for a 42° range of movement is 3.20° ± 1.20° for able-bodied, while it is 3.40° ± 0.26° for paraplegic subjects. The results demonstrate that the proposed control strategy provides system dynamics with an invariance property to model uncertainties and subject-to-subject variations. Figure 7 shows that there is a low-level co-activation at the low activation levels. The level of agonist–antagonist co-activation tends to decrease as the muscle activation increases.

4.2.1. Muscle fatigue compensation. Figure 8 shows the ability of the ARC to compensate the muscle fatigue for the biphasic raised-cosine and trapezoidal trajectories. The average of the RMS error is about 3.6° for the raised-cosine trajectory and 3.2° for the trapezoidal trajectory over 3 min. The results show that the method could adjust the stimulation pattern to compensate the muscle fatigue and the tracking performance remains fairly constant throughout the trial. The shift to higher stimulation levels over the course of session indicates muscle fatigue. It is observed that the level of co-contraction changes during different cycles of movement. An interesting observation is the presence of symmetry in a stimulation pattern of agonist and antagonist muscles.

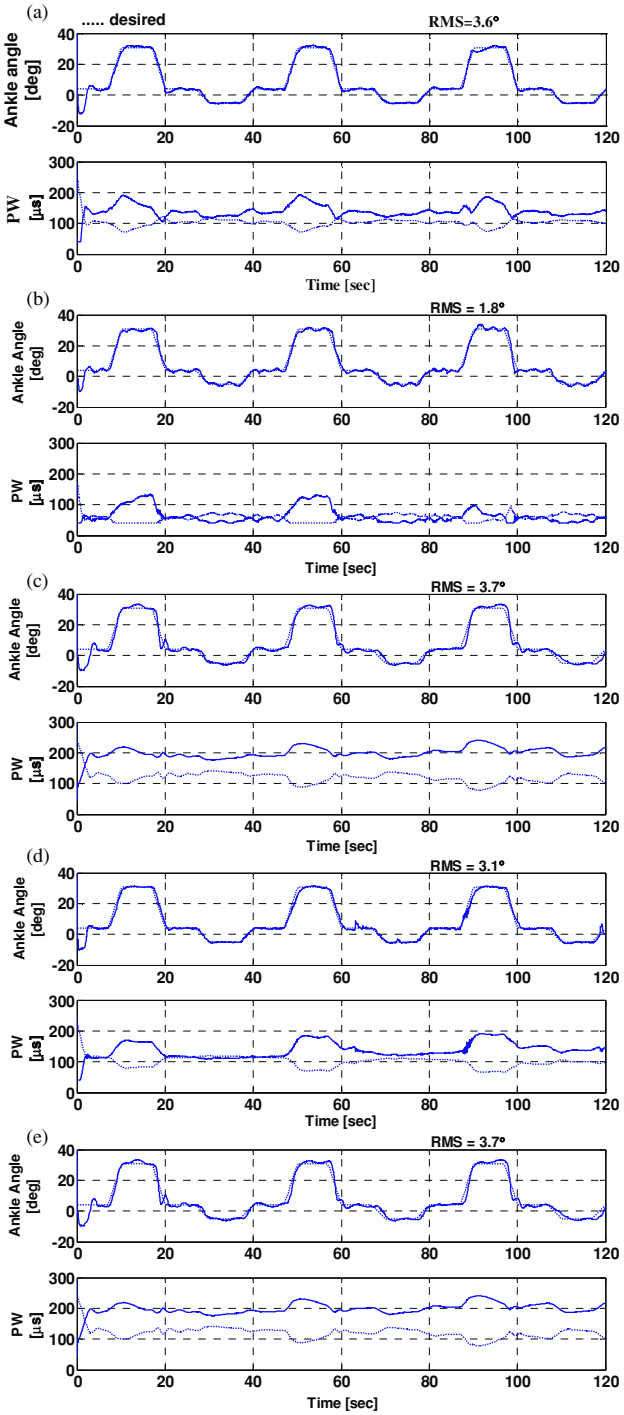

Figure 7. Typical results of controlling dorsiflexion and plantarflexion movements on healthy subjects KM (a), NH (b) and AS (c), and paraplegic subjects MH (d), and MS (e) using the ARC ($k = 50, \phi = 5, \lambda = 3$). The bottom plots in (a)–(e) show the control signals of dorsiflexor (solid) and plantarflexor (dotted) muscles.

Comparing the results obtained during prolonged stimulation (figure 8) with that obtained during short stimulation (figure 7), it is observed that the RMS tracking errors are almost the same. This observation clearly demonstrates the robustness of ARC against the time-varying property of the muscle-joint dynamics.

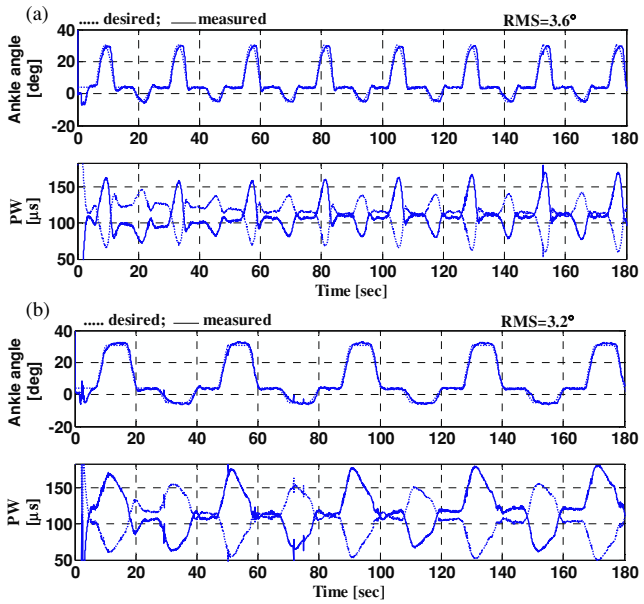

Figure 8. The ability of the proposed SMC ($k = 50, \phi = 5, \lambda = 3$) to compensate the muscle fatigue for two different desired movement trajectories on paraplegic subject RR. The bottom plots in (a), (b) show the control signals of dorsiflexor (solid) and plantarflexor (dotted) muscles.

Table 2. Summary of the average daily root-mean-square tracking error (±standard deviation) obtained for paraplegic subjects using the ARC.

Subject	Day 1	Day 2	Day 3
MS	$3.81^\circ \pm 0.70^\circ$	$4.46^\circ \pm 0.42^\circ$	$4.90^\circ \pm 0.61^\circ$
MH	$5.31^\circ \pm 0.46^\circ$	$5.17^\circ \pm 0.45^\circ$	$5.48^\circ \pm 0.56^\circ$
RR	$3.20^\circ \pm 0.20^\circ$	$3.40^\circ \pm 0.20^\circ$	$3.50^\circ \pm 0.50^\circ$
Mean		$3.40^\circ \pm 0.20^\circ$	

4.2.2. Effects of external disturbances. Figure 9(a) shows a typical result of an external disturbance rejection using ARC in paraplegic subject MH. The disturbance was realized by gently putting a load (1.0 kg) on the ankle at $t = 79$ s and removing it at $t = 141$ s. It is observed that a perfect disturbance rejection is obtained through the proposed SMC (RMS error 5.5°). Another typical result of a mechanical disturbance to the musculoskeletal system for the sine-wave trajectory in paraplegic subject MS is shown in figure 9(b) (RMS error 7.04°). The controller could adjust the stimulation pattern such that a perfect disturbance rejection is achieved. The interesting observation is the fast convergence speed of the tracking trajectory at the time of applying the disturbance. In these experiments, we also used the same values for the model parameters which were determined during the first day of experiment on one healthy subject and adapting the parameters of nonlinear compensator was performed online without any offline training.

5. Discussion and conclusion

In previous work [28], a robust control strategy was designed which was based on the synergistic combination of artificial

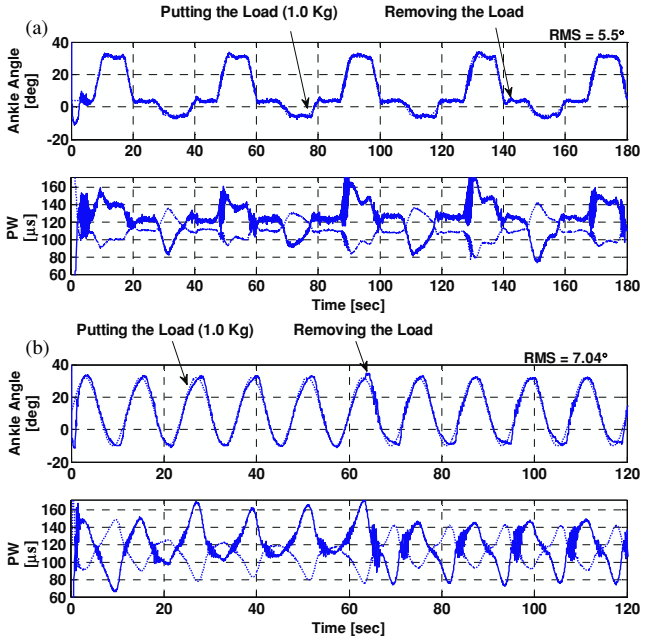

Figure 9. Effect of an external disturbance rejection using the proposed SMC ($k = 50, \phi = 5, \lambda = 3$) in paraplegic subjects MH (a) and MS (b). The bottom plots in (a), (b) show the control signals of dorsiflexor (solid) and plantarflexor (dotted) muscles.

neural networks with sliding mode control (SMC) for controlling *the knee-joint angle* using quadriceps muscle stimulation. To eliminate the chattering, we coupled two neural networks with online learning without any offline training into the SMC. Although the controller provides an excellent tracking performance with no chattering for single muscle group stimulation, the online computation burden to update the parameters of neural networks is not appropriate for multi-actuator and multi-joint movement. The work presented in this paper is concerned with developing a new robust control strategy resulting in a simpler design whereas the controller performance is not obviously degraded. Unlike the previous study, the method proposed in the current study is designed for controlling the multiple muscle system, i.e. ankle dorsiflexion and plantarflexion.

Extensive simulation studies on a virtual patient and experiments on healthy and paraplegic subjects demonstrate the exceptional performance and robustness of the proposed control strategy during system parameter variations, muscle fatigue and external disturbances. The results clearly indicate that the proposed SMC makes system motion robust with respect to the time-varying properties of musculoskeletal dynamics, day-to-day and subject-to-subject variations. This result is achieved without using any subject-specific model information. The control system does not require any re-identification of the plant model during different experiment sessions and even for applying the controller on a new subject. The parameters of the model were identified using the data obtained during the first experiment session of one healthy subject. Then, the values of identified parameters are used for subsequent experiment sessions on different days for all subjects. The adaptation of the adaptive compensator

was performed *online* during *online control* without offline training.

The results show that the average NRMS tracking error is 7.8% (RMS error 3.3°) over all subjects while Jezernik *et al* [27] who used a sliding mode control for controlling the knee-joint angle by stimulating the quadriceps muscle reported an average tracking error of 23.8%.

Another important feature of the proposed method is that the state trajectories can be controlled to achieve fast convergence. The ankle movement trajectory converges to the desired trajectory after about 2 s. This observation is the direct consequence of the exponential convergence rate of the tracking error in the SMC. In contrast, an adaptive control is able to achieve only asymptotic convergence. Asymptotic stability implies that the system trajectories converge to the equilibrium as time goes to infinity. For example, Abbas *et al* [17] who used an adaptive feedforward controller for controlling the knee-joint angle by stimulating the quadriceps muscle group reported that the tracking error for the first few cycles was very large and reduced to within 10% after an average of 30 cycles (75 s). In [14], the results of an adaptive control of single-joint movement by stimulating the quadriceps muscle showed that the controller took more than 20 s to converge.

One striking feature of the proposed control system is the ability to control the interaction between agonist and antagonist muscles without preprogramming the concurrent agonist–antagonist activities. The results show that there is a low-level co-activation at the low force levels. Furthermore, the simulation studies show that the level of agonist–antagonist co-activation increases during the fatiguing state and loaded condition.

In this work, we proposed a robust method for the control of agonist and antagonist activities in the ankle. Future work will focus on exploitation of this strategy for the control of unsupported standing in paraplegia using FES.

Appendix

Brief introduction to sliding mode control (SMC)

Consider the following nonlinear system

$$\ddot{x} = f(x,t) + g(x,t)\cdot u(t) + \mathrm{d}(t) \tag{A.1}$$

where $x(t)$ is the state to be controlled so that it follows a desired trajectory $x_d(t)$, $d(t)$ is the external disturbances which are unknown but bounded by the known function, i.e. $|d(t)| \leqslant D$ and $u(t)$ is the control input. The nonlinear dynamics $f(x,t)$ and the control gain $g(x,t)$ are not known exactly, but are estimated as the known nominal dynamics $\hat{f}(x,t)$ and $\hat{g}(x,t)$, respectively, with the bounded estimation errors. With uncertainties, the dynamic equation of the system (A.1) can be modified as

$$\begin{aligned}\ddot{x} &= (f(x,t) + \Delta f(x,t)) + (g(x,t) + \Delta g(x,t))\cdot u(t) + d(t)\\ &= f(x,t) + g(x,t)\cdot u(t) + \mathrm{w}(x,t)\end{aligned} \tag{A.2}$$

where $\Delta f(x,t)$ and $\Delta g(x,t)$ denote unmodeled dynamics and parameter uncertainties; $w(x,t)$ is the lumped uncertainty and defined as

$$w(x,t) = \Delta f(x,t) + \Delta g(x,t)\cdot u(t) + d(t). \tag{A.3}$$

Here the bound of the lumped uncertainty is assumed to be given, that is

$$|w(x,t)| < v. \tag{A.4}$$

The objective of the controller is to design a control law to force the system state vector to track a desired state vector in the presence of model uncertainties and external disturbances. We first define a sliding surface as follows:

$$s(e,t) = \left(\frac{d}{\mathrm{d}t} + \lambda\right)^2 \left(\int_0^t e(r)\,\mathrm{d}r\right) = 0 \tag{A.5}$$

where $e(t)$ is the state error and λ is a positive constant. By solving the above equation for the control input using (A.1), we obtain the following expression for $u(t)$ which is called the equivalent control, u_{eq}:

$$\begin{aligned}u_{\mathrm{eq}}(t) &= \frac{1}{\hat{g}(x,t)}\cdot(-\hat{f}(x) + \ddot{x}_d(t) - 2\lambda\dot{e}(t) - \lambda^2 e(t))\\ &= \frac{1}{\hat{g}(x,t)}\cdot\hat{u}(t).\end{aligned} \tag{A.6}$$

The equivalent control keeps the system states in the sliding surface $s = 0$ if the dynamics were exactly known. Hence, if the state is outside the sliding surface, to drive the state to the sliding surface, we choose the control law such that

$$\frac{1}{2}\frac{\mathrm{d}}{\mathrm{d}t}s^2 \leqslant -\eta\,|s|\,, \tag{A.7}$$

where η is a strictly positive constant and (A.7) is called the reaching condition. The control objective is to guarantee that the state trajectory can converge to the sliding surface. It can be proved that the control law

$$u_1(t) = \frac{1}{\hat{g}(x,t)}\cdot[\hat{u}(t) - k\cdot\mathrm{sgn}(s)] \tag{A.8}$$

with $k \geqslant v + \eta$ satisfies the sliding condition (A.7) [44].

This control law leads to high-frequency control switching and chattering across sliding surface. The chattering caused by the high-frequency switching control activity is highly undesirable and is not acceptable for the control of functional electrical stimulation and may excite unmodeled high-frequency plant dynamics which could result in unpredictable instability. To overcome this problem, the SMC strategy deserves special attention, because this method provides a systematic approach to maintain asymptotic stability and consistent performance.

References

[1] Prochazka A, Gauthier M, Wieler M and Kenwell K 1997 The bionic glove: an electrical stimulator garment that provides controlled grasp and hand opening in quadriplegia *Arch. Phys. Med. Rehabil.* **78** 608–14

[2] Peckham P H *et al* 2001 Efficacy of an implanted neuroprosthesis for restoring hand grasp in tetraplegia: a multicenter study *Arch. Phys. Med. Rehabil.* **82** 1380–8

[3] Memberg W D, Crago P E and Keith M W 2003 Restoration of elbow extension via functional electrical stimulation in individuals with tetraplegia *J. Rehabil. Res. Dev.* **40** 477–86

[4] Graupe D, Davis R, Kordylewski H and Kohn K H 1998 Ambulation by traumatic T4–T12 paraplegics using functional neuromuscular stimulation *Crit. Rev. Neurosurg.* **8** 221–31

[5] Agarwal S, Triolo R J, Kobetic R, Miller M, Bieri C, Kukke S, Rohde L and Davis J A 2003 Long-term user perceptions of an implanted neuroprosthesis for exercise, standing, and transfers after spinal cord injury *J. Rehabil. Res. Dev.* **40** 241–52

[6] Lyons G M, Sinkjær T, Burridge J H and Wilcox D J 2002 A review of portable FES-based neural orthoses for the correction of drop foot *IEEE Trans. Neural Syst. Rehabil. Eng.* **10** 260–79

[7] Abbas J J and Chizeck H J 1991 Feedback control of coronal plane hip angle in paraplegic subjects using functional neuromuscular stimulation *IEEE Trans. Biomed. Eng.* **38** 687–98

[8] Lan N, Crago P E and Chizeck H J 1991 Control of end-point forces of multi joint limb by functional electrical stimulation *IEEE Trans. Biomed. Eng.* **38** 935–65

[9] Bernotas L A, Crago P E and Chizeck H J 1987 Adaptive control of electrically stimulated muscle *IEEE Trans. Biomed. Eng.* **34** 140–7

[10] Hatwell M S, Oderkerk B J, Sacher C A and Inbar G F 1991 The development of a model reference adaptive controller to control the knee joint of paraplegics *IEEE Trans. Autom. Control* **36** 683–91

[11] Abbas J J and Chizeck H J 1991 Feedback control methods for task regulation by electrical stimulation of muscle *IEEE Trans. Biomed. Eng.* **38** 1213–23

[12] Previdi F and Carpanzano E 2003 Design of a gain scheduling controller for knee-joint angle control by using functional electrical stimulation *IEEE Trans. Control Syst. Technol.* **11** 310–24

[13] Chang G-C, Lub J-J, Liao G-D, Lai J-S, Cheng C-K, Kuo B-L and Kuo T-S 1997 A neuro-control system for the knee joint position control with quadriceps stimulation *IEEE Trans. Rehabil. Eng.* **5** 2–11

[14] Ferrarin M, Palazzo F, Riener R and Quintern J 2001 Model-based control of FES-induced single joint movements *IEEE Neural Syst. Rehabil.* **9** 245–57

[15] Abbas J J and Chizeck H J 1995 Neural network control of functional neuromuscular stimulation systems *IEEE Trans. Biomed. Eng.* **42** 1117–27

[16] Abbas J J and Triolo R J 1993 Experimental evaluation of an adaptive feedforward controller for use in functional neuromuscular stimulation systems *Proc. 15th Annual Conf. Int. Engineering in Medicine and Biology Society*

[17] Riess J and Abbas J J 2000 Adaptive neural network control of cyclic movements using functional neuromuscular stimulation *IEEE Trans. Rehabil. Eng.* **8** 42–52

[18] Riess J and Abbas J J 2001 Adaptive control of cyclic movements as muscles fatigue using functional neuromuscular stimulation *IEEE Trans. Neural Syst. Rehabil.* **9** 326–30

[19] Mirizarandi A R, Erfanian A and Kobravi H R 2005 Adaptive Inverse control of knee joint position in paraplegic subjects using recurrent neural network *Proc. 10th Ann. Conf. Int. Functional Electrical Stimulation Society.*

[20] Kurosawa K, Futami R, Watanabe T and Hoshimiya N 2005 Joint angle control by FES using a feedback error learning controller *IEEE Trans. Neural Syst. Rehabil.* **13** 359–71

[21] Hongliu D and Nair S S 1998 Learning control design for a class of nonlinear systems *Eng. Appl. Artif. Intell.* **11** 495–505

[22] Zhang T, Ge S S, Hang C C and Chai T Y 2000 Adaptive control of first-order systems with nonlinear parameterization *IEEE Trans. Autom. Control* **45** 1512–6

[23] Miller D E 2003 A new approach to model reference adaptive control *IEEE Trans. Autom. Control* **48** 743–57

[24] Slotine J J E and Li W 1991 *Applied Nonlinear Control* (Englewood Cliffs, NJ: Prentice-Hall)

[25] Young K D, Utkin V I and Özgüner Ü 1999 A control engineer's guide to sliding mode control *IEEE Trans. Control Syst. Technol.* **7** 328–42

[26] Guldner J and Utkin V I 2000 The chattering problem in sliding mode systems *Proc. 14th Int. Symp. of Mathematical Theory of Networks and Systems (MTNS)*

[27] Jezernik S, Wassink R G V and Keller T 2004 Sliding mode closed-loop control of FES: controlling the shank movement *IEEE Trans. Biomed. Eng.* **51** 263–72

[28] Ajoudani A and Erfanian A 2009 A neuro-sliding mode control with adaptive modeling of uncertainty for control of movement in paralyzed limbs using functional electrical stimulation *IEEE Trans. Biomed. Eng.* **56** 1771–80

[29] Ebrahimpour M M and Erfanian A 2008 Comments on sliding mode closed-loop control of FES: controlling the shank movement *IEEE Trans. Biomed. Eng.* **55** 2842–3

[30] Lister S J, Jones N B, Spurgeon S K and Scott J J A 2006 Simulation of human gait and associated muscle activation strategies using sliding-mode control techniques *Simul. Modelling Pract. Theory* **14** 586–96

[31] Mohammad S, Fraisse P, Guiraud D, Poignet P and Makssoud H E 2005 Towards a co-contraction muscle control strategy for paraplegics *Proc. 44th Ann. IEEE Conf. Robotics and Automation*

[32] Levant A 2001 Universal single-input-single-output (SISO) sliding-mode controllers with finite-time convergence *IEEE Trans. Autom. Control* **9** 1447–51

[33] Zhou B-H, Baratta R V, Solomonow M, Olivier L J, Nguyen G T and D'Ambrosia R D 1996 Evaluation of isometric antagonist coactivation strategies of electrically stimulated muscles *IEEE Trans. Biomed. Eng.* **43** 150–60

[34] Zhou B-H, Katz S R, Baratta R V, Solomonow M and D'Ambrosia R D 1997 Evaluation of antagonist coactivation strategies elicited from electrically stimulated muscles under load-moving conditions *IEEE Trans. Biomed. Eng.* **44** 620–33

[35] Matjačić Z and Bajd T 1998 Arm-free paraplegic standing: Part I: Control model synthesis and simulation *IEEE Trans. Rehabil. Eng.* **6** 125–38

[36] Popović D, Stein R B, Oğuztöreli N, Lebiedowska M and Jonić S 1999 Optimal control of walking with functional electrical stimulation: a computer simulation study *IEEE Trans. Rehabil. Eng.* **7** 69–79

[37] Soetanto D, Kuo C Y and Babic D 2001 Stabilization of human standing posture using functional neuromuscular stimulation *J. Biomech.* **34** 1589–97

[38] Mihelj M and Munih M 2004 Unsupported standing with minimized ankle muscle fatigue *IEEE Trans. Biomed. Eng.* **51** 1330–40

[39] Seraji H and Bajd T 1989 Decentralized adaptive control of manipulators: theory, simulation, and experimentation *IEEE Trans. Robot. Autom.* **5** 183–201

[40] Chang W-D, Hwang R-C and Hsieh J-G 2002 Application of an auto-tuning neuron to sliding mode control *IEEE Trans. Syst. Man Cybern.* C **32** 517–22

[41] Wang L-X 1997 *A Course in Fuzzy Systems and Control* (Englewood Cliffs, NJ: Prentice-Hall)

[42] Kobravi H R and Erfanian A 2004 A transcutaneous computer-based closed-loop motor neuroprosthesis for real-time movement control *Proc. 9th Ann. Conf. Int. Functional Electrical Stimulation Society*

[43] Erfanian A, Kobravi H R, Zohorian O and Emani F 2006 A portable programmable transcutaneous neuroprosthesis with built-in self-test capability for training and mobility in paraplegic subjects *Proc. 11th Ann. Conf. Int. Functional Electrical Stimulation Society*

[44] Yu W-S and Chen Y-H 2005 Decoupled variable structure control design for trajectory tracking on mechatronic arms *IEEE Trans. Control Syst. Technol* **13** 798–806